Research Article

Azzh Saad Alshehry, Humaira Yasmin*, Rasool Shah, Roman Ullah, and Asfandyar Khan

Fractional-order modeling: Analysis of foam drainage and Fisher's equations

https://doi.org/10.1515/phys-2023-0115
received August 18, 2023; accepted September 11, 2023

Abstract: In this study, we use a dual technique that combines the Laplace residual power series method (LRPSM) and the new iteration method, both of which are combined with the Caputo operator. Our primary goal is to solve two unique but difficult partial differential equations: the foam drainage equation and the nonlinear time-fractional Fisher's equation. These equations, which are crucial in modeling complex processes, confront analytical complications, owing to their fractional derivatives and nonlinear behavior. We develop exact and efficient solutions by merging these unique methodologies, which are supported by thorough figures and tables that demonstrate the precision and trustworthiness of our methodology. We not only shed light on the solutions to these equations, but also demonstrate the prowess of the LRPSM and the new iteration method as powerful tools for grappling with complex mathematical and physical models, significantly contributing to advancements in various scientific domains.

Keywords: foam drainage equation, nonlinear time-fractional Fisher's equation, Laplace residual power series method, new iteration method, Caputo operator, fractional order differential equation

*** Corresponding author: Humaira Yasmin**, Department of Basic Sciences, Preparatory Year Deanship, King Faisal University, Al-Ahsa, 31982, Saudi Arabia, e-mail: hhassain@kfu.edu.sa
Azzh Saad Alshehry: Department of Mathematical Sciences, Faculty of Sciences, Princess Nourah Bint Abdulrahman University, P.O. Box 84428, Riyadh 11671, Saudi Arabia, e-mail: asalshihry@pnu.edu.sa
Rasool Shah: Department of Mathematics, Abdul Wali University Mardan, Khyber Pakhtunkhwa, Pakistan, e-mail: rasoolshahawkum@gmail.com
Roman Ullah: Department of General Studies, Higher Colleges of Technology, Dubai Women Campus, United Arab Emirates, e-mail: romanullah@yahoo.com
Asfandyar Khan: Department of Mathematics, Abdul Wali University Mardan, Khyber Pakhtunkhwa, Pakistan, e-mail: asfandyarmath@awkum.edu.pk

1 Introduction

Most physical events and problems in science are nonlinear. Finding accurate analytical answers to such issues is challenging, with just a small number of exceptions. So, many have tried to develop novel methods of obtaining analytical answers that are relatively close to the precise solutions [1]. Hirota's bilinear method [2], the homogeneous balance method [3,4], the inverse scattering method [5], Adomian's decomposition method (ADM) [6,7], the variational iteration method [8,9], the d-expansion method [10–12], and the homotopy analysis method (HAM) have all gained significant attention in recent years. To begin, in 1992, Liao proposed a broad analytic technique for nonlinear problems using the fundamental principle of homotopy from topology [13–16]. Then, the HAM was used to resolve a wide variety of nonlinear problems [17–22].

The foam drainage equation is given as:

$$\frac{\partial \psi(\nu,\sigma)}{\partial \sigma} = \frac{\partial}{\partial \nu}\left(\psi^2(\nu,\sigma) - \frac{\sqrt{\psi(\nu,\sigma)}}{2}\frac{\partial \psi(\nu,\sigma)}{\partial \nu}\right), \quad (1)$$

where ν and σ are the scaled position and time coordinates, respectively, and the initial condition is as follows:

$$\psi(\nu,\sigma) = p(\nu). \quad (2)$$

Numerous everyday activities, both natural and man-made, depend on foam. Foam has attracted a lot of attention in academic studies because of their uses; thus, both scientists and everyday individuals are highly familiar with them [23–25]. Foods and personal care items such as creams and lotions often include foams. Cleaning and scrubbing textiles often produce foam [26]. They have significant uses in the chemical and food sectors, as well as in the processing of minerals, combating fires, and structural material sciences [27].

Fisher introduced the Fisher–Kolmogorov–Petrovsky–Piskunov (Fisher-KPP) equation [28] before renaming it Fisher equation. Fractional equations have numerous applications in the engineering and scientific communities [29–32]. Important generalizations of this equation were studied by the researchers [33–35]. Numerous reaction–diffusion equations use wavefronts

to explain chemical, physical, and biological phenomena [36,37]. Population dynamics in advective environments [38] are characterized by the Fisher-KPP advection equation. The nonlinear partial Fisher equation is given as:

$$\frac{\partial \psi(\nu, \sigma)}{\partial \sigma} = \frac{\partial^2 \psi(\nu, \sigma)}{\partial \nu^2} + \psi(\nu, \sigma)(1 - \psi(\nu, \sigma)). \tag{3}$$

As a model for gene selection, Fisher presented Eq. (3), where $\psi(\nu, \sigma)$ denotes the population density. Autocatalytic chemistry, nuclear reactor theory, flame dynamics, neurophysiology, and Brownian motion all use the same equation. The Fisher equation is often used in engineering and is hence considered a significant equation.

The Laplace residual power series method (LRPSM) and new iterative method (NIM) are used to solve these equations in this study. A complex mathematical method for solving variable coefficient ordinary differential equations (ODEs) and partial differential equations (PDEs) is the LRPSM [42–45]. This method uses the Laplace transform (LT) and power series approaches to solve a class of ODEs and PDEs that are difficult to solve using normal methods. Translating complex and nonlinear differential equations into a LT form and extending the expression into a power series allow for the systematic solution estimation. In circumstances when direct analytical solutions are unavailable, LRPSM helps researchers and professionals gain deeper insights into a broad variety of dynamic systems across varied areas [46–48].

The invention of an iterative technique for fractional partial differential equations advances mathematical analysis and problem resolution. When solving fractional derivative partial differential equations, traditional methods often struggle with convergence and processing complexity. This innovative iterative technique refines approximation solutions to improve accuracy while maintaining computational economy to overcome these limits. This approach may provide improved answers for complex mathematical and physical phenomena by iteration to fractional derivative features [49–51]. It helps us model and understand complicated fractional partial differential equation-governed systems in physics, engineering, and applied mathematics. The LRPSM and NIM are effective methods for solving fractional differential equations, providing immediate and visible symbolic terms and numerically approximate solutions without linearization or discretization. This study aimed to solve the foam drainage problem and the nonlinear time-fractional Fisher's equation using LRPSM and NIM and compare their performance. The reader should know that these two strategies have solved many nonlinear fractional differential problems.

2 Basic definitions

2.1 Definition

The derivative of a function of order p that is not an integer is defined by the Caputo [39]:

$$^{C}D_{\sigma}^{m}\psi(\nu, \sigma) = \frac{1}{\Gamma(m-p)}\int_{0}^{\sigma}(\sigma - \vartheta)^{m-p-1}\psi^{(m)}(\nu, \vartheta)\mathrm{d}\vartheta, \quad m - 1 < \alpha \le m, \quad t > 0. \tag{4}$$

2.2 Definition

The expression for the noninteger Riemann integral is given in the study of El-Tantawy *et al.* [40] as:

$$\Re_{\sigma}^{p}\psi(\nu, \sigma) = \frac{1}{\Gamma(p)}\int_{0}^{\sigma}(\sigma - \vartheta)^{p-1}\psi(\nu, \vartheta)\mathrm{d}\vartheta. \tag{5}$$

2.3 Definition

The LT of $\psi(\nu, \sigma)$ is presented in the study of El-Ajou [39]:

$$\psi(\varsigma, s) = \mathcal{L}_{\sigma}[\psi(\nu, \sigma)] = \int_{0}^{\infty} e^{-s\sigma}\psi(\nu, \tau)\mathrm{d}\sigma, \ \ s > p. \tag{6}$$

The following is the definition for the inverse LT:

$$\begin{aligned}\psi(\nu, \sigma) &= \mathcal{L}_{\sigma}^{-1}[\psi(\nu, s)] \\ &= \int_{b-i\infty}^{b+i\infty} e^{s\sigma}\psi(\nu, s)\mathrm{d}s, b = \mathrm{Re}(s) > b_0.\end{aligned} \tag{7}$$

2.4 Lemma

For $n - 1 < k \le n$, $\zeta > -1$, $\rho \ge 0$, and $\omega \in R$, we have:

(1) $D_{\sigma}^{k}\sigma^{\omega} = \frac{\Gamma(k+1)}{\Gamma(\omega-k+1)}\sigma^{\omega-k}$,

(2) $D_{\sigma}^{k}\rho = 0$,

(3) $D_{\sigma}^{k}\Re_{\sigma}^{k}\psi(\nu, \sigma) = \psi(\nu, \sigma)$,

(4) $\Re_{\sigma}^{k}D_{\sigma}^{k}\psi(\nu, \sigma) = \psi(\nu, \sigma) - \sum_{i=0}^{n-1}\partial^{i}\psi(\nu, 0)\frac{\sigma^{i}}{i!}$.

3 Road map of the proposed methods

3.1 General procedure of LRPSM

Take into account the fractional-order partial differential equation:

$$D_\sigma^p \psi(\nu,\sigma) + N[\psi(\nu,\sigma)] + R[\psi(\nu,\sigma)] = 0, \quad \text{where } 0 < p \le 1, \tag{8}$$

subject to initial condition:

$$\psi(\nu,0) = f_0(\nu), \tag{9}$$

where $N[\psi(\nu,\sigma)]$ denotes a nonlinear operator, whereas $R[\psi(\nu,\sigma)]$ constitutes the linear component.

Upon using the LT on Eq. (8) and incorporating Eq. (9), we obtain

$$\psi(\nu,s) - \frac{f_0(\nu,s)}{s} + \frac{1}{s^p}\mathcal{L}_\sigma[N[\mathcal{L}_\sigma^{-1}[\psi(\nu,s)]]] + \frac{1}{s^p}R[\psi(\nu,s)] = 0. \tag{10}$$

Let Eq. (11) be the solution to Eq. (10):

$$\psi(\nu,s) = \sum_{n=0}^{\infty} \frac{f_n(\nu,s)}{s^{np+1}}, \tag{11}$$

and the kth-truncated term series are

$$\psi(\nu,s) = \frac{f_0(\nu,s)}{s} + \sum_{n=1}^{k} \frac{f_n(\nu,s)}{s^{np+1}}, \quad n = 1,2,3,4,\ldots \tag{12}$$

The Laplace residual functions (LRFs) [41] are

$$\mathcal{L}_\sigma \mathrm{Res}(\nu,s) = \psi(\nu,s) - \frac{f_0(\nu,s)}{s} + \frac{1}{s^p}\mathcal{L}_\sigma[N[\mathcal{L}_\sigma^{-1}[\psi(\nu,s)]]] + \frac{1}{s^p}R[\psi(\nu,s)], \tag{13}$$

and the kth-LRFs are as follows:

$$\mathcal{L}_\sigma \mathrm{Res}_k(\nu,s) = \psi_k(\nu,s) - \frac{f_0(\nu,s)}{s} + \frac{1}{s^p}\mathcal{L}_\sigma[N[\mathcal{L}_\sigma^{-1}[\psi_k(\nu,s)]]] + \frac{1}{s^p}R[\psi_k(\nu,s)]. \tag{14}$$

The following LRPSM characteristics are listed in order to emphasize various aspects:

- $\mathcal{L}_\sigma \mathrm{Res}(\nu,s) = 0$ and $\lim_{j\to\infty} \mathcal{L}_\sigma \mathrm{Res}_k(\nu,s) = \mathcal{L}_\sigma \mathrm{Res}_\nu(\nu,s)$ for each $s > 0$.
- $\lim_{s\to\infty} s\mathcal{L}_\sigma \mathrm{Res}_\nu(\nu,s) = 0 \Rightarrow \lim_{s\to\infty} s\mathcal{L}_\sigma \mathrm{Res}_{\nu,k}(\nu,s) = 0$.
- $\lim_{s\to\infty} s^{kp+1}\mathcal{L}_\sigma \mathrm{Res}_{\nu,k}(\nu,s) = \lim_{s\to\infty} s^{kp+1}\mathcal{L}_\sigma \mathrm{Res}_{\nu,k}(\nu,s) = 0$, $0 < p \le 1$, $k = 1,2,3,\ldots$.

The following system is recursively solved to obtain the coefficients using $f_n(\nu,s)$:

$$\lim_{s\to\infty} s^{kp+1}\mathcal{L}_\sigma \mathrm{Res}_{\nu,k}(\nu,s) = 0, \quad k = 1,2,\ldots. \tag{15}$$

Finally, apply the inverse LT to Eq. (11) to obtain the kth analytical result of $\psi_k(\nu,\sigma)$.

3.2 Analysis of NIM

To grasp the fundamental concept of the novel iterative technique, we consider the general functional equation:

$$\psi(\nu) = f(\nu) + N(\psi(\nu)), \tag{16}$$

where N represents a nonlinear operator mapping from a Banach space B to B and f denotes an unknown function; our pursuit has been focused on finding a solution to (16) that takes the form of a series:

$$\psi(\nu) = \sum_{i=0}^{\infty} \psi_i(\nu). \tag{17}$$

The nonlinear term can be decomposed as:

$$N\left(\sum_{i=0}^{\infty}\psi_i(\nu)\right) = N(\psi_0(\nu)) + \sum_{i=0}^{\infty} \times \left[N\left(\sum_{j=0}^{i}\psi_j(\nu)\right) - N\left(\sum_{j=0}^{i-1}\psi_j(\nu)\right)\right]. \tag{18}$$

From (16), (17), and (18), it is equivalent to:

$$\sum_{i=0}^{\infty}\psi_i(\nu) = f(\nu) + N(\psi_0(\nu)) + \sum_{i=0}^{\infty} \times \left[N\left(\sum_{j=0}^{i}\psi_j(\nu)\right) - N\left(\sum_{j=0}^{i-1}\psi_j(\nu)\right)\right]. \tag{19}$$

The recurrence relation is defined as:

$$\begin{aligned} \psi_0(\nu) &= f(\nu), \\ \psi_1(\nu) &= N(\psi_0(\nu)), \\ \psi_2(\nu) &= N(\psi_0(\nu) + \psi_1(\nu)) - N(\psi_0(\nu)), \\ \psi_{n+1}(\nu) &= N(\psi_0(\nu) + \psi_1(\nu) + \cdots \psi_n) \\ &\quad - N(\psi_0(\nu) + \psi_1(\nu) + \cdots \psi_{n-1}(\nu)), \\ &\quad n = 1,2,3,\ldots \end{aligned} \tag{20}$$

Then,

$$\begin{aligned}&(\psi_0(\nu)+\psi_1(\nu)+\cdots\psi_n(\nu))\\&\quad=N(\psi_0(\nu)+\psi_1(\nu)+\cdots\psi_n(\nu)),\ n=1,2,3,\ldots,\\&\psi(\nu)=\sum_{i=0}^{\infty}\psi_i(\nu)=f(\nu)+N\left(\sum_{i=0}^{\infty}\psi_i(\nu)\right).\end{aligned}\tag{21}$$

3.2.1 Basic road map of NIM

Here, we will explore the basics of using the NIM to solve fractional-order nonlinear partial differential equations. Take a look at the following equation for a partial differential in the fractional order:

$$D_\sigma^p\psi(\nu,\sigma)=A(\psi,\partial\psi)+\sigma(x,t),\ m-1<p\le m,\ m\in N,\tag{22}$$

$$\frac{\partial^k}{\partial t^k}\psi(\nu,0)=h_k(\nu),\ k=0,1,2,3,\ldots,m-1,\tag{23}$$

where A is nonlinear function of ψ and $\partial\psi$ (partial derivative of ψ with respect to ν and σ) and B is the source function. In view of the NIM, the intimal value problems (22) and (23) are equivalent to the integral equation:

$$\psi(\nu,\sigma)=\sum_{k=0}^{m-1}h_k(\nu)\frac{t^k}{k!}+\Re_\sigma^p(A)+\Re_\sigma^p(\sigma)=f+N(\psi),\tag{24}$$

where

$$f=\sum_{k=0}^{m-1}h_k(\nu)\frac{\sigma^k}{k!}+\Re_\sigma^p(\sigma),\tag{25}$$

$$N(\psi)=\Re_\sigma^p(A).\tag{26}$$

Problem 1

Consider the time-fractional Fisher's equation is given as:

Implementation of LRPSM

$$\begin{aligned}&D_\sigma^p\psi(\nu,\sigma)-\frac{\partial^2\psi(\nu,\sigma)}{\partial\nu^2}-\psi(\nu,\sigma)+\psi^7(\nu,\sigma)\\&\quad=0,\ \text{where } 0<p\le1.\end{aligned}\tag{27}$$

Subjected to the following ICs:

$$\psi(\nu,0)=\frac{1}{\left(1+e^{\frac{3\nu}{2}}\right)^{\frac{1}{3}}},\tag{28}$$

having the exact solution:

$$\psi(\nu,\sigma)=\sqrt[3]{\left\{\frac{1}{2}\tanh\left(\frac{15\sigma}{8}-\frac{3\nu}{4}\right)+\frac{1}{2}\right\}}.$$

Applying LT to Eq. (27) and making use of Eq. (28), we obtain

$$\begin{aligned}&\psi(\nu,s)-\frac{\frac{1}{\left(1+e^{\frac{3\nu}{2}}\right)^{\frac{1}{3}}}}{s}-\frac{1}{s^p}\frac{\partial^2\psi(\nu,s)}{\partial\nu^2}\\&\quad-\frac{1}{s^p}\psi(\nu,s)+\frac{1}{s^p}\mathcal{L}_\sigma[(\mathcal{L}_\sigma^{-1}[\psi(\nu,s)])^7]=0,\end{aligned}\tag{29}$$

and so the kth-truncated term series are as follows:

$$\psi(\nu,s)=\frac{\frac{1}{\left(1+e^{\frac{3\nu}{2}}\right)^{\frac{1}{3}}}}{s}+\sum_{r=1}^{k}\frac{f_r(\nu,s)}{s^{rp+1}},\ r=1,2,3,4,\ldots.\tag{30}$$

LRFs [41] are as follows:

$$\begin{aligned}\mathcal{L}_\sigma\mathrm{Res}(\nu,s)=\psi(\nu,s)&-\frac{\frac{1}{\left(1+e^{\frac{3\nu}{2}}\right)^{\frac{1}{3}}}}{s}\\&-\frac{1}{s^p}\frac{\partial^2\psi(\nu,s)}{\partial\nu^2}-\frac{1}{s^p}\psi(\nu,s)\\&+\frac{1}{s^p}\mathcal{L}_\sigma[(\mathcal{L}_\sigma^{-1}[\psi(\nu,s)])^1]=0,\end{aligned}\tag{31}$$

and the kth-LRFs are as follows:

$$\begin{aligned}\mathcal{L}_\sigma\mathrm{Res}_k(\nu,s)=\psi_k(\nu,s)&-\frac{\frac{1}{\left(1+e^{\frac{3\nu}{2}}\right)^{\frac{1}{3}}}}{s}-\frac{1}{s^p}\frac{\partial^2\psi_k(\nu,s)}{\partial\nu^2}\\&-\frac{1}{s^p}\psi_k(\nu,s)+\frac{1}{s^p}\mathcal{L}_\sigma[(\mathcal{L}_\sigma^{-1}[\psi_k(\nu,s)])^7]\\&=0.\end{aligned}\tag{32}$$

Now, to determine $f_r(\nu,s)$, $r=1,2,3,\ldots$, we substitute the rth-truncated series Eq. (30) into the rth-LRF Eq. (32), multiply the resulting equation by s^{rp+1}, and then solve recursively the relation $\lim_{s\to\infty}(s^{rp+1}\mathcal{L}_\sigma\mathrm{Res}_{\psi,r}(\nu,s))=0$, $r=1,2,3,\ldots$. Following are the first few terms:

$$f_1(\nu,s)=\frac{5e^{\frac{3\nu}{2}}}{4\left(e^{\frac{3\nu}{2}}+1\right)^{4/3}},\tag{33}$$

$$f_2(\nu,s)=\frac{25e^{3\nu}-75e^{\frac{3\nu}{2}}}{16\left(e^{\frac{3\nu}{2}}+1\right)^{7/3}},\tag{34}$$

and so on.

Putting the values of $f_r(v,s)$, $r = 1, 2, 3, \ldots$, in Eq. (30), we obtain

$$\psi(v,s) = \frac{1}{s}\left(\frac{1}{\left(1+e^{\frac{3v}{2}}\right)^{1/3}}\right) + \frac{1}{s^{p+1}}\left(\frac{5e^{\frac{3v}{2}}}{4\left(e^{\frac{3v}{2}}+1\right)^{4/3}}\right) + \frac{1}{s^{2p+1}}\left(\frac{25e^{3v}-75e^{\frac{3v}{2}}}{16\left(e^{\frac{3v}{2}}+1\right)^{7/3}}\right)+\cdots. \tag{35}$$

Using inverse LT, we obtain (Figure 1)

$$\psi(v,\sigma) = \frac{1}{\left(1+e^{\frac{3v}{2}}\right)^{1/3}} + \frac{\sigma^p}{\Gamma(p+1)}\left(\frac{5e^{\frac{3v}{2}}}{4\left(e^{\frac{3v}{2}}+1\right)^{4/3}}\right) + \frac{\sigma^{2p}}{\Gamma(2p+1)}\left(\frac{25e^{3v}-75e^{\frac{3v}{2}}}{16\left(e^{\frac{3v}{2}}+1\right)^{7/3}}\right)+\cdots. \tag{36}$$

Implementation of NIM

Applying RL integral to Eq. (27), we obtain the equivalent form:

$$\psi(v,\sigma) = \frac{1}{\left(1+e^{\frac{3v}{2}}\right)^{\frac{1}{3}}} - \Re_\sigma^p\left[\frac{\partial^2\psi(v,\sigma)}{\partial v^2} + \psi(v,\sigma) - \psi^7(v,\sigma)\right]. \tag{37}$$

According to the NIM procedure, we obtain the following few terms:

$$\begin{aligned}
&\psi_0(v,\sigma) = \frac{1}{\left(1+e^{\frac{3v}{2}}\right)^{\frac{1}{3}}}, \psi_1(v,\sigma) = \frac{5e^{\frac{3v}{2}}\sigma^p}{4\left(e^{\frac{3v}{2}}+1\right)^{4/3}\Gamma(p+1)},\\
&\psi_2(v,\sigma) = \frac{25e^{\frac{3v}{2}}\sigma^{2p}}{131{,}072\left(e^{\frac{3v}{2}}+1\right)^{28/3}} \times \left(-\frac{120{,}000\,e^{\frac{15v}{2}}\left(e^{\frac{3v}{2}}+1\right)\sigma^{5p}\Gamma(6p)}{\Gamma(7p)\Gamma(p+1)^6} - \frac{2{,}1875\,e^{9v}\sigma^{6p}\Gamma(7p)}{\Gamma(8p)\Gamma(p+1)^7} + 64\left(e^{\frac{3v}{2}}+1\right)^2\right.\\
&\quad\times\left(-\frac{5{,}600\,e^{\frac{9v}{2}}\left(e^{\frac{3v}{2}}+1\right)\sigma^{3p}\Gamma(4p)}{\Gamma(5p)\Gamma(p+1)^4} - \frac{4{,}375\,e^{6v}\sigma^{4p}\Gamma(5p)}{\Gamma(6p)\Gamma(p+1)^5} + 8\left(e^{\frac{3v}{2}}+1\right)^2\right.\\
&\quad\left.\left.\times\left(-\frac{525e^{3v}\sigma^{2p}\Gamma(3p)}{\Gamma(4p)\Gamma(p+1)^3} - \frac{336e^{\frac{3v}{2}}\left(e^{\frac{3v}{2}}+1\right)\sigma^p\Gamma(2p+1)}{\Gamma(p+1)^2\Gamma(3p+1)} + \frac{16\left(e^{\frac{3v}{2}}-3\right)\left(e^{\frac{3v}{2}}+1\right)^3}{\Gamma(2p+1)}\right)\right)\right).
\end{aligned} \tag{38}$$

By the NIM algorithm, the final solution is under (Figure 2):

$$\psi(v,\sigma) = \psi_0(v,\sigma) + \psi_1(v,\sigma) + \psi_2(v,\sigma) + \cdots, \tag{39}$$

$$\psi(v,\sigma)=\frac{1}{\left(1+e^{\frac{3v}{2}}\right)^{\frac{1}{3}}}+\frac{5e^{\frac{3v}{2}}\sigma^{p}}{4\left(e^{\frac{3v}{2}}+1\right)^{4/3}\Gamma(p+1)}+\frac{25e^{\frac{3v}{2}}\sigma^{2p}}{131{,}072\left(e^{\frac{3v}{2}}+1\right)^{28/3}}\Bigg(-\frac{120{,}000\,e^{\frac{15v}{2}}\left(e^{\frac{3v}{2}}+1\right)\sigma^{5p}\Gamma(6p)}{\Gamma(7p)\Gamma(p+1)^{6}}$$
$$-\frac{21{,}875\,e^{9v}\sigma^{6p}\Gamma(7p)}{\Gamma(8p)\Gamma(p+1)^{7}}+64\left(e^{\frac{3v}{2}}+1\right)^{2}\Bigg(-\frac{5{,}600\,e^{\frac{9v}{2}}\left(e^{\frac{3v}{2}}+1\right)\sigma^{3p}\Gamma(4p)}{\Gamma(5p)\Gamma(p+1)^{4}} \tag{40}$$
$$-\frac{4{,}375\,e^{6v}\sigma^{4p}\Gamma(5p)}{\Gamma(6p)\Gamma(p+1)^{5}}+8\left(e^{\frac{3v}{2}}+1\right)^{2}\times\Bigg(-\frac{525e^{3v}\sigma^{2p}\Gamma(3p)}{\Gamma(4p)\Gamma(p+1)^{3}}$$
$$-\frac{336e^{\frac{3v}{2}}\left(e^{\frac{3v}{2}}+1\right)\sigma^{p}\Gamma(2p+1)}{\Gamma(p+1)^{2}\Gamma(3p+1)}+\frac{16\left(e^{\frac{3v}{2}}-3\right)\left(e^{\frac{3v}{2}}+1\right)^{3}}{\Gamma(2p+1)}\Bigg)\Bigg)\Bigg).$$

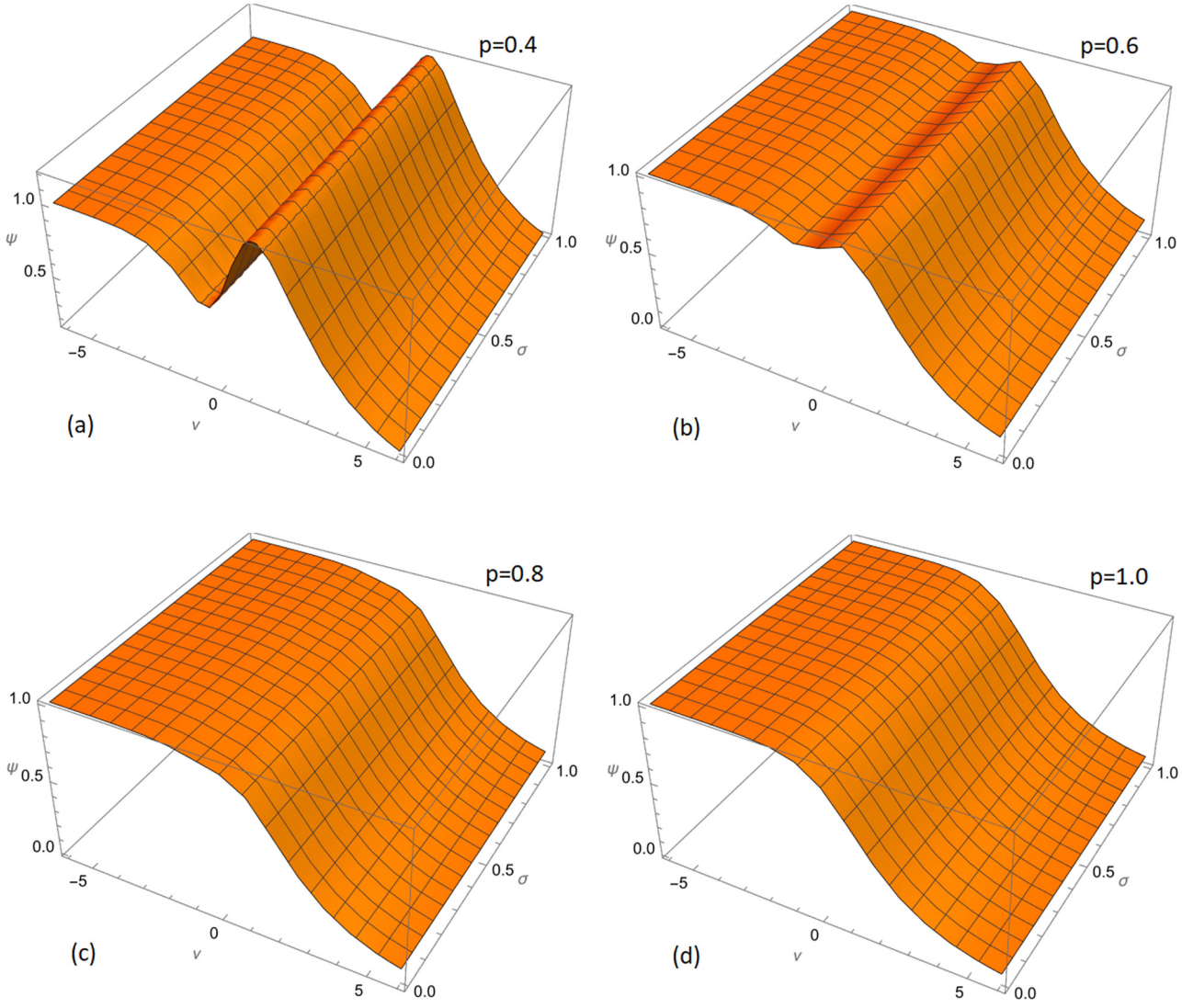

Figure 1: (a) Fractional order 0.4, (b) fractional order 0.6, (c) fractional order 0.8, and (d) fractional order 1.0, of LRPSM of Example 1 for $\sigma = 0.1$.

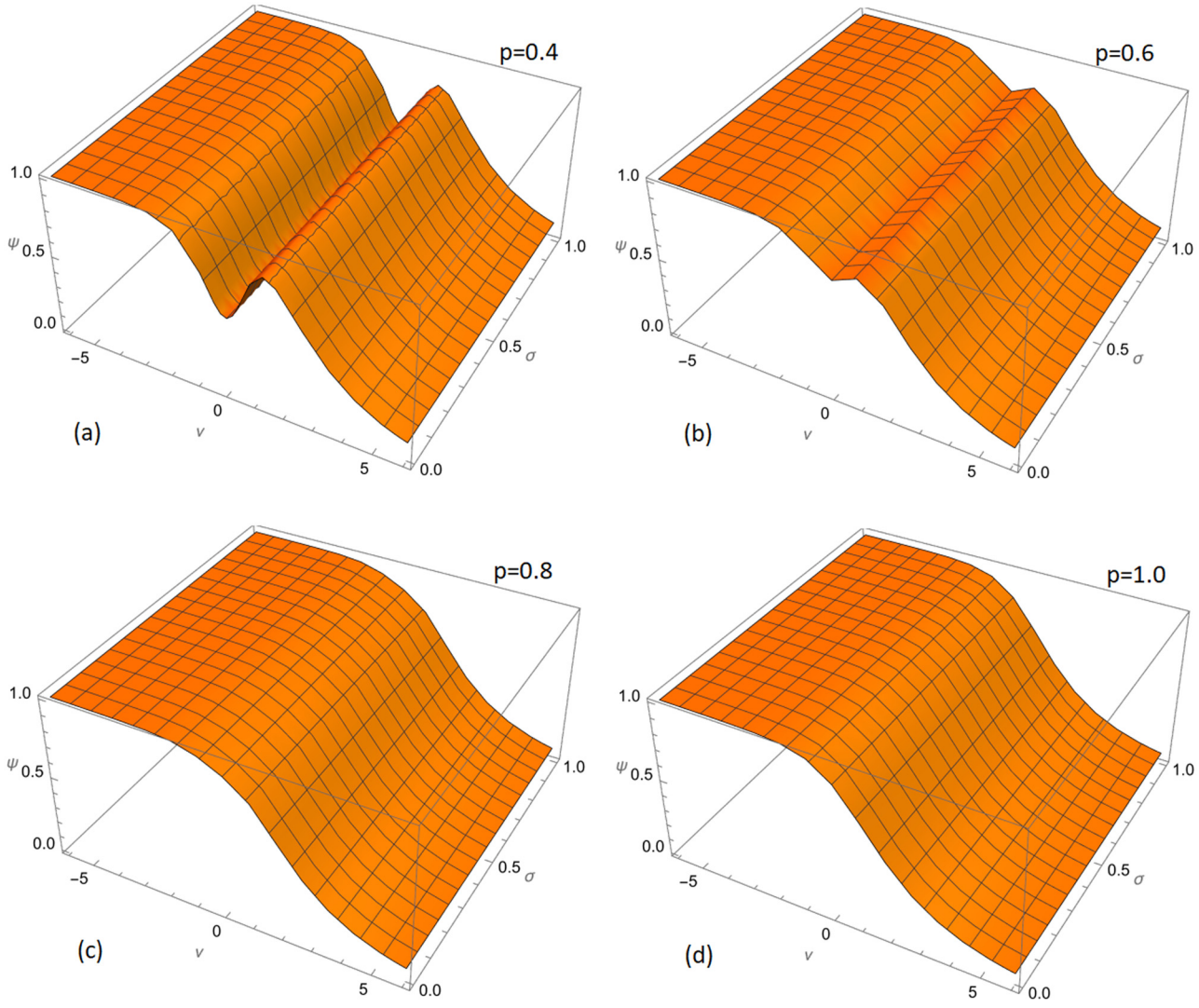

Figure 2: (a) Fractional order 0.4, (b) fractional order 0.6, (c) fractional order 0.8, and (d) fractional order 1.0, of NIM of Example 1 for $\sigma = 0.01$.

Note the impact of $p = 0.4$, $p = 0.5$, $p = 0.6$, $p = 0.8$, and $p = 1.0$ when comparing the results from the LRPSM and the NIM for Example 1. As the fractional order p approaches 1, the previously observed jagged response becomes more smooth. This demonstrates that solutions of higher fractional orders tend to be more uniform and smooth. Extensive computational study has been assigned to improving the precision of the approaches used in Example 1. The meticulously compiled results of these computations are shown in Tables 1–4. This neatly compiled data set provides substantial evidence for the convergence behavior and overall accuracy of the selected approaches.

Problem 2

Consider the time-fractional foam drainage is given as:

Implementation of LRPSM

$$D_{\sigma}^{p}\psi(\nu,\sigma) - \frac{\psi(\nu,\sigma)\partial^{2}\psi(\nu,\sigma)}{2\partial\nu^{2}} + 2\psi^{2}(\nu,\sigma)\frac{\partial\psi(\nu,\sigma)}{\partial\nu} - \left(\frac{\partial\psi(\nu,\sigma)}{\partial\nu}\right)^{2} = 0, \quad \text{where } 0 < p \le 1. \tag{41}$$

Subjected to the following ICs:

Table 1: Comparison of different fractional orders of LRPSM of Example 1 for $\sigma = 0.1$

v	$\text{LRPSM}_{P=0.6}$	$\text{LRPSM}_{p=0.8}$	$\text{LRPSM}_{P=1.0}$	Exact	$\text{Error}_{p=0.6}$	$\text{Error}_{p=0.8}$	$\text{Error}_{p=1.0}$
0.	0.897646	0.867218	0.840206	0.839982	0.057664	0.027236	0.000224085
0.1	0.887814	0.852086	0.822573	0.822297	0.0655173	0.0297891	0.000276224
0.2	0.876862	0.835753	0.803816	0.803496	0.0733664	0.0322569	0.000319893
0.3	0.864665	0.818237	0.78401	0.783657	0.0810075	0.0345792	0.000352936
0.4	0.851123	0.799581	0.763254	0.76288	0.0882427	0.0367008	0.000374043
0.5	0.836175	0.779857	0.741665	0.741282	0.0948932	0.038575	0.000382832
0.6	0.819803	0.759159	0.719373	0.718993	0.10081	0.0401661	0.000379812
0.7	0.802035	0.737605	0.696521	0.696155	0.105881	0.0414504	0.000366238
0.8	0.782947	0.71533	0.673257	0.672913	0.110034	0.0424172	0.000343897
0.9	0.762654	0.692483	0.649731	0.649416	0.113238	0.0430672	0.00031487
1.	0.741302	0.669216	0.626086	0.625805	0.115497	0.0434112	0.000281305

Table 2: Comparison of different fractional orders of LRPSM of Example 1 for $\sigma = 0.01$

v	$\text{LRPSM}_{P=0.6}$	$\text{LRPSM}_{p=0.8}$	$\text{LRPSM}_{P=1.0}$	Exact	$\text{Error}_{p=0.6}$	$\text{Error}_{p=0.8}$	$\text{Error}_{p=1.0}$
0.	0.82649	0.806805	0.79863	0.79863	0.0278597	0.00817548	2.551131×10^{-7}
0.1	0.808072	0.787147	0.778547	0.778547	0.0295251	0.00860059	3.030978×10^{-7}
0.2	0.788602	0.766533	0.757553	0.757553	0.0310494	0.00898002	3.412176×10^{-7}
0.3	0.768171	0.745076	0.735769	0.735769	0.0324017	0.00930665	3.677563×10^{-7}
0.4	0.746886	0.722904	0.713329	0.713329	0.0335566	0.00957517	3.819198×10^{-7}
0.5	0.724872	0.700158	0.690377	0.690376	0.0344957	0.00978222	3.838502×10^{-7}
0.6	0.702266	0.676984	0.667058	0.667057	0.0352083	0.0099265	3.745207×10^{-7}
0.7	0.679209	0.653527	0.643518	0.643518	0.0356912	0.0100086	3.555417×10^{-7}
0.8	0.655849	0.629932	0.619901	0.619901	0.0359484	0.010031	3.289235×10^{-7}
0.9	0.632328	0.606335	0.596338	0.596338	0.0359899	0.00999731	2.968351×10^{-7}
1.	0.608783	0.582864	0.572952	0.572952	0.0358309	0.00991246	2.613958×10^{-7}

$$\psi(v, 0) = \frac{1}{2e^{v} + 1} - \frac{1}{2}. \tag{42}$$

$$\psi(v, \sigma) = \frac{1}{2e^{v - \frac{\sigma}{4}} + 1} - \frac{1}{2}. \tag{43}$$

The exact solution is as follows:

Applying LT to Eq. (41) and making use of Eq. (42), we obtain

Table 3: Comparison of different fractional orders of NIM of Example 1 for $\sigma = 0.1$

v	$\text{NIM}_{P=0.6}$	$\text{NIM}_{p=0.8}$	$\text{NIM}_{P=1.0}$	Exact	$\text{Error}_{p=0.6}$	$\text{Error}_{p=0.8}$	$\text{Error}_{p=1.0}$
0.	0.87018	0.863079	0.839619	0.839982	0.0301978	0.0230968	0.000363059
0.1	0.860823	0.848054	0.822004	0.822297	0.0385263	0.0257568	0.000292883
0.2	0.850977	0.831919	0.803277	0.803496	0.0474812	0.0284232	0.000218503
0.3	0.840434	0.814678	0.783513	0.783657	0.0567763	0.0310207	0.000144358
0.4	0.828973	0.796355	0.762806	0.76288	0.0660921	0.0334746	0.0000746898
0.5	0.816388	0.776997	0.741269	0.741282	0.0751058	0.0357157	0.0000130628
0.6	0.802513	0.756679	0.719031	0.718993	0.0835205	0.0376864	0.0000379655
0.7	0.787243	0.735498	0.696232	0.696155	0.0910884	0.0393438	0.0000770026
0.8	0.77054	0.713575	0.673017	0.672913	0.0976263	0.0406618	0.000103793
0.9	0.752437	0.691046	0.649535	0.649416	0.103021	0.0416304	0.000119045
1.	0.733031	0.66806	0.625929	0.625805	0.107226	0.0422547	0.000124174

Table 4: Comparison of different fractional orders of NIM of Example 1 for $\sigma = 0.01$

v	$\text{NIM}_{p=0.6}$	$\text{NIM}_{p=0.8}$	$\text{NIM}_{p=1.0}$	Exact	$\text{Error}_{p=0.6}$	$\text{Error}_{p=0.8}$	$\text{Error}_{p=1.0}$
0.	0.826131	0.806791	0.79863	0.79863	0.0275011	0.00816089	2.917156×10^{-7}
0.1	0.807725	0.787133	0.778547	0.778547	0.0291779	0.00858652	2.240841×10^{-7}
0.2	0.788274	0.76652	0.757553	0.757553	0.0307214	0.00896676	1.548604×10^{-7}
0.3	0.767868	0.745063	0.735769	0.735769	0.032099	0.00929446	8.806200×10^{-8}
0.4	0.746613	0.722893	0.713329	0.713329	0.0332838	0.00956421	2.730880×10^{-8}
0.5	0.724632	0.700149	0.690376	0.690376	0.0342553	0.00977259	2.455687×10^{-8}
0.6	0.702058	0.676975	0.667057	0.667057	0.035001	0.00991821	6.570495×10^{-8}
0.7	0.679034	0.65352	0.643518	0.643518	0.035516	0.0100017	9.538290×10^{-8}
0.8	0.655704	0.629926	0.619901	0.619901	0.035803	0.0100252	1.138263×10^{-7}
0.9	0.632209	0.60633	0.596338	0.596338	0.0358715	0.00999261	1.220580×10^{-7}
1.	0.608688	0.582861	0.572952	0.572952	0.035736	0.0099087	1.216313×10^{-7}

$$\begin{aligned}\psi(v,s) - \frac{\frac{1}{2e^{v}+1} - \frac{1}{2}}{s} \\ - \frac{1}{2s^{p}}\mathfrak{L}_{\sigma}\left[(\mathfrak{L}_{\sigma}^{-1}\psi(v,s))\left(\mathfrak{L}_{\sigma}^{-1}\frac{\partial^{2}\psi(v,s)}{2\partial v^{2}}\right)\right] \\ + \frac{2}{s^{p}}\mathfrak{L}_{\sigma}\left[(\mathfrak{L}_{\sigma}^{-1}\psi^{2}(v,s))\left(\mathfrak{L}_{\sigma}^{-1}\frac{\partial\psi(v,s)}{\partial v}\right)\right] \\ - \mathfrak{L}_{\sigma}\left[\left(\mathfrak{L}_{\sigma}^{-1}\frac{\partial\psi v,s}{\partial v}\right)^{2}\right] = 0,\end{aligned} \tag{44}$$

and so the kth-truncated term series are as follows:

$$\psi(v,s) = \frac{\frac{1}{2e^{v}+1} - \frac{1}{2}}{s} + \sum_{r=1}^{k}\frac{f_{r}(v,s)}{s^{rp+1}},\ r = 1,2,3,4,\ldots. \tag{45}$$

LRFs [41] are as follows:

$$\begin{aligned}\mathcal{L}_{\sigma}\text{Res}(v,s) = \psi(v,s) - \frac{\frac{1}{2e^{v}+1} - \frac{1}{2}}{s} - \frac{1}{2s^{p}}\mathfrak{L}_{\sigma} \\ \times\left[(\mathfrak{L}_{\sigma}^{-1}\psi(v,s)) \times (\mathfrak{L}_{\sigma}^{-1}\frac{\partial^{2}\psi(v,s)}{2\partial v^{2}})\right] \\ + \frac{2}{s^{p}}\mathfrak{L}_{\sigma}\left[(\mathfrak{L}_{\sigma}^{-1}\psi^{2}(v,s))(\mathfrak{L}_{\sigma}^{-1}\frac{\partial\psi(v,s)}{\partial v})\right] \\ - \mathfrak{L}_{\sigma}[(\mathfrak{L}_{\sigma}^{-1}\frac{\partial\psi v,s}{\partial v})^{2}] = 0,\end{aligned} \tag{46}$$

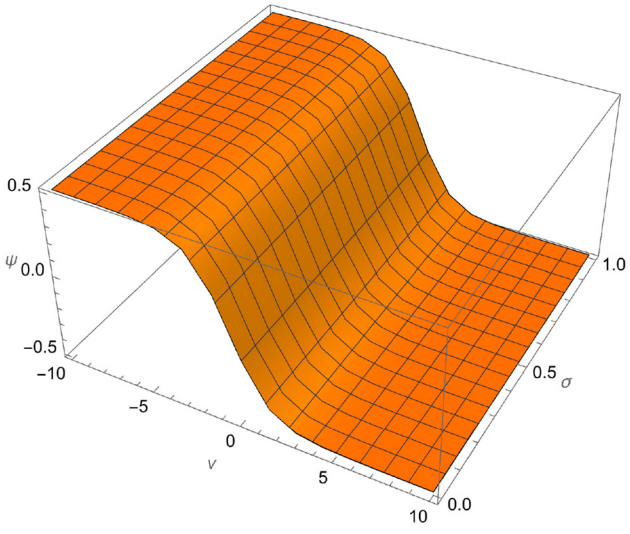

Figure 3: Approximate solution of LRPSM of Example 2 for $\sigma = 0.5$ and $p = 1$.

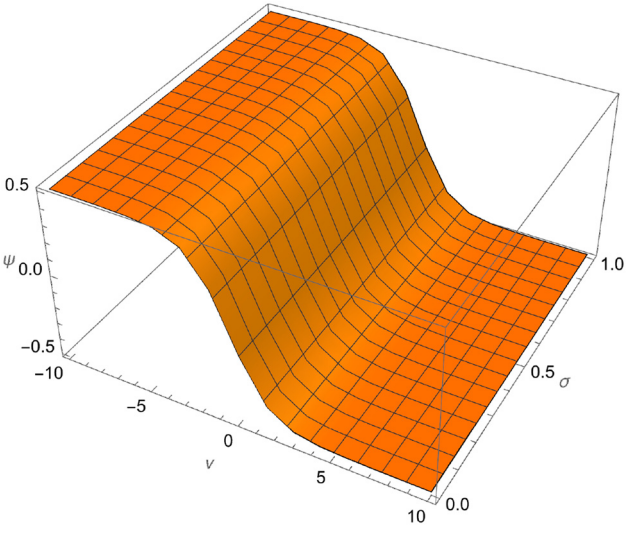

Figure 4: Exact solution of Example 2 for $\sigma = 0.5$.

and the kth-LRFs are as follows:

$$\begin{aligned}\mathcal{L}_\sigma \mathrm{Res}_k(v,s) &= \psi_k(v,s) - \frac{\frac{1}{2e^v+1}-\frac{1}{2}}{s} - \frac{1}{2s^p}\mathfrak{L}_\sigma \\ &\times \left[(\mathfrak{L}_\sigma^{-1}\psi_k(v,s)) \times \left(\mathfrak{L}_\sigma^{-1}\frac{\partial^2\psi_k(v,s)}{2\partial v^2}\right)\right] \\ &+ \frac{2}{s^p}\mathfrak{L}_\sigma[(\mathfrak{L}_\sigma^{-1}\psi_k^2(v,s)) \\ &\times \left(\mathfrak{L}_\sigma^{-1}\frac{\partial\psi_k(v,s)}{\partial v}\right)\Bigg] \\ &- \mathfrak{L}_\sigma\left[\left(\mathfrak{L}_\sigma^{-1}\frac{\partial\psi_k(v,s)}{\partial v}\right)^2\right] = 0.\end{aligned} \tag{47}$$

Now, to determine $f_r(v,s)$, $r = 1, 2, 3, \ldots$, we substitute the rth-truncated series Eq. (45) into the rth-LRF Eq. (47), multiply the resulting equation by s^{rp+1}, and then solve recursively the relation $\lim_{s\to\infty}(s^{rp+1}\mathcal{L}_\sigma \mathrm{Res}_{\psi,r}(v,s)) = 0, r = 1, 2, 3, \ldots$. Following are the first few terms:

$$f_1(v,s) = \frac{e^v}{2(2e^v+1)^2}, \tag{48}$$

$$f_2(v,s) = \frac{e^v(2e^v-1)}{8(2e^v+1)^3}, \tag{49}$$

and so on.

Putting the values of $f_r(v,s)$, $r = 1, 2, 3, \ldots$, in Eq. (45), we obtain

$$\begin{aligned}\psi(v,s) = \frac{\frac{1}{2e^v+1}-\frac{1}{2}}{s} &+ \frac{1}{4s^{p+1}}\left(\frac{e^v}{2(2e^v+1)^2}\right) \\ &+ \frac{1}{16s^{2p+1}}\left(\frac{e^v(2e^v-1)}{8(2e^v+1)^3}\right) + \cdots.\end{aligned} \tag{50}$$

Using inverse LT, we obtain (Figures 3 and 4)

$$\begin{aligned}\psi(v,\sigma) = \frac{1}{2e^v+1} - \frac{1}{2} &+ \frac{\sigma^p}{\Gamma(p+1)}\left(\frac{e^v}{2(2e^v+1)^2}\right) \\ &+ \frac{\sigma^{2p}}{\Gamma(2p+1)}\left(\frac{e^v(2e^v-1)}{8(2e^v+1)^3}\right) + \cdots.\end{aligned} \tag{51}$$

Implementation of NIM

Applying RL integral to Eq. (41), we obtain the equivalent form:

$$\begin{aligned}\psi(v,\sigma) = \frac{1}{2e^v+1} - \frac{1}{2} - \Re_\sigma^p\Bigg[&\frac{\psi(v,\sigma)\partial^2\psi(v,\sigma)}{2\partial v^2} \\ &- 2\psi^2(v,\sigma)\frac{\partial\psi(v,\sigma)}{\partial v} + \left(\frac{\partial\psi(v,\sigma)}{\partial v}\right)^2\Bigg].\end{aligned} \tag{52}$$

According to the NIM procedure, we obtain the following few terms:

$$\begin{aligned}\psi_0(v,\sigma) &= \frac{1}{2e^v+1} - \frac{1}{2}, \\ \psi_1(v,\sigma) &= \frac{e^v\sigma^p}{2(2e^v+1)^2\Gamma(p+1)}, \\ \psi_2(v,\sigma) &= \frac{e^v\sigma^{2p}}{8(2e^v+1)^7}\Bigg(\frac{2e^{2v}(2e^v-1)\sigma^{2p}\Gamma(3p+1)}{\Gamma(p+1)^3\Gamma(4p+1)} \\ &- \frac{e^v(2e^v+1)(4e^v(e^v-2)+1)\sigma^p\Gamma(2p+1)}{\Gamma(p+1)^2\Gamma(3p+1)} \\ &+ \frac{(2e^v-1)(2e^v+1)^4}{\Gamma(2p+1)}\Bigg).\end{aligned} \tag{53}$$

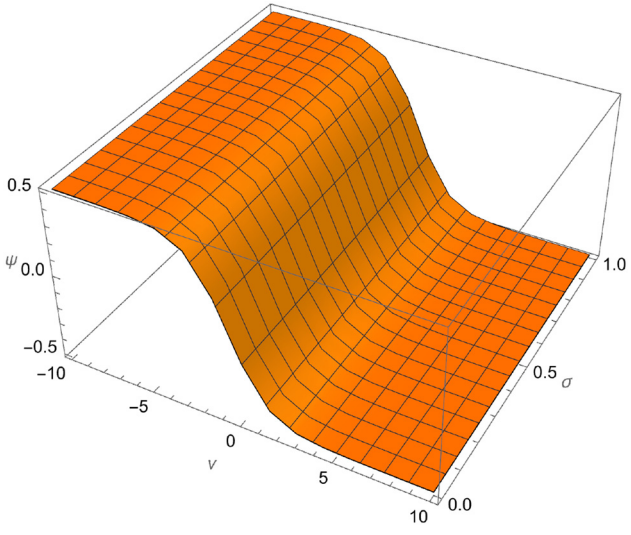

Figure 5: Approximate solution of NIM of Example 2 for $\sigma = 0.5$ and $p = 1$.

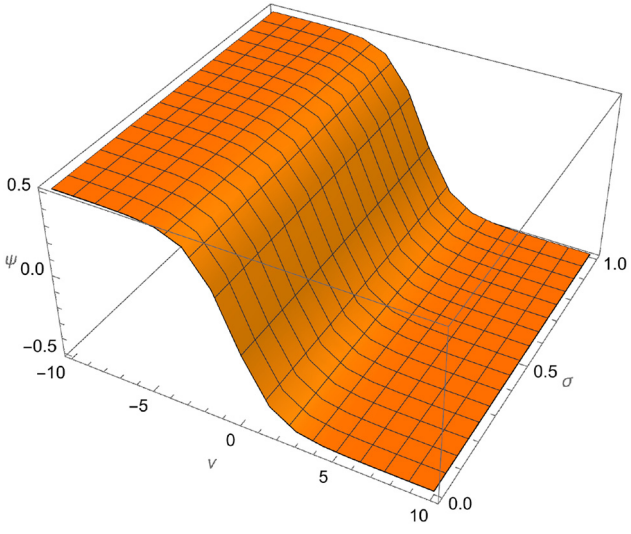

Figure 6: Exact solution of Example 2 for $\sigma = 0.5$.

Table 5: Comparison of different fractional orders of LRPSM of Example 2 for $\sigma = 0.5$

v	LRPSM$_{p=0.6}$	LRPSM$_{p=0.8}$	LRPSM$_{p=1.0}$	Exact	Error$_{p=0.6}$	Error$_{p=0.8}$	Error$_{p=1.0}$
0.	−0.120025	−0.127617	−0.13831	−0.138336	0.0183106	0.0107182	0.0000253517
0.1	−0.1432	−0.150642	−0.161067	−0.161088	0.0178878	0.0104463	0.0000213093
0.2	−0.165731	−0.172987	−0.183103	−0.18312	0.0173895	0.0101328	0.0000171672
0.3	−0.187535	−0.194577	−0.204347	−0.20436	0.016825	0.00978334	0.0000130459
0.4	−0.208545	−0.215346	−0.224741	−0.22475	0.0162047	0.00940405	9.0523198×10^{-6}
0.5	−0.228705	−0.235243	−0.244239	−0.244244	0.0155392	0.00900106	5.2762681×10^{-6}
0.6	−0.247971	−0.25423	−0.262808	−0.26281	0.0148389	0.00858041	1.788482×10^{-6}
0.7	−0.266311	−0.272277	−0.280427	−0.280425	0.014114	0.00814792	1.359778×10^{-6}
0.8	−0.283707	−0.289372	−0.297085	−0.297081	0.0133741	0.00770903	4.136010×10^{-6}
0.9	−0.300148	−0.305507	−0.312782	−0.312776	0.012628	0.00726869	6.524802×10^{-6}
1.	−0.315635	−0.320688	−0.327528	−0.327519	0.0118839	0.00683135	8.525544×10^{-6}

Table 6: Comparison of different fractional orders of LRPSM of Example 2 for $\sigma = 0.1$

v	LRPSM$_{p=0.6}$	LRPSM$_{p=0.8}$	LRPSM$_{p=1.0}$	Exact	Error$_{p=0.6}$	Error$_{p=0.8}$	Error$_{p=1.0}$
0.	−0.14638	−0.154319	−0.161088	−0.161088	0.0147081	0.00676921	1.949057×10^{-7}
0.1	−0.16887	−0.176571	−0.18312	−0.18312	0.0142502	0.00654873	1.622431×10^{-7}
0.2	−0.190615	−0.198052	−0.20436	−0.20436	0.0137454	0.00630772	1.290341×10^{-7}
0.3	−0.211548	−0.2187	−0.22475	−0.22475	0.0132017	0.00604999	9.622055×10^{-8}
0.4	−0.231617	−0.238465	−0.244244	−0.244244	0.0126275	0.00577934	6.462600×10^{-8}
0.5	−0.250779	−0.25731	−0.26281	−0.26281	0.0120307	0.00549949	3.493203×10^{-8}
0.6	−0.269006	−0.275211	−0.280425	−0.280425	0.0114193	0.00521397	7.665638×10^{-8}
0.7	−0.28628	−0.292155	−0.297081	−0.297081	0.0108005	0.00492606	1.680170×10^{-8}
0.8	−0.302595	−0.308137	−0.312776	−0.312776	0.0101809	0.00463874	3.824605×10^{-8}
0.9	−0.317953	−0.323165	−0.327519	−0.327519	0.00956647	0.00435465	5.657611×10^{-8}
1.0	−0.332366	−0.337253	−0.341329	−0.341329	0.00896243	0.00407608	7.181400×10^{-8}

Table 7: Comparison of different fractional orders of NIM of Example 2 for $\sigma = 0.5$

v	NIM$_{p=0.5}$	NIM$_{p=0.7}$	NIM$_{p=1.0}$	Exact	Error$_{p=0.5}$	Error$_{p=0.7}$	Error$_{p=1.0}$
0.	−0.119823	−0.127525	−0.138287	−0.138336	0.0185121	0.0108106	0.0000485713
0.1	−0.143033	−0.150566	−0.161048	−0.161088	0.0180552	0.0105226	0.0000403011
0.2	−0.165597	−0.172927	−0.183088	−0.18312	0.0175231	0.0101932	0.0000320415
0.3	−0.187433	−0.194531	−0.204336	−0.20436	0.0169268	0.00982881	0.0000240568
0.4	−0.208473	−0.215314	−0.224733	−0.22475	0.0162773	0.00943591	0.0000165629
0.5	−0.228658	−0.235223	−0.244235	−0.244244	0.015586	0.00902092	9.721501×10^{-6}
0.6	−0.247946	−0.25422	−0.262806	−0.26281	0.0148635	0.00859006	3.640295×10^{-6}
0.7	−0.266305	−0.272276	−0.280427	−0.280425	0.0141203	0.00814918	1.623050×10^{-6}
0.8	−0.283715	−0.289377	−0.297087	−0.297081	0.0133659	0.00770365	6.054432×10^{-6}
0.9	−0.300167	−0.305517	−0.312785	−0.312776	0.0126088	0.00725832	9.675106×10^{-6}
1.	−0.315663	−0.320702	−0.327532	−0.327519	0.0118567	0.00681744	0.000012533

Table 8: Comparison of different fractional orders of NIM of Example 2 for $\sigma = 0.1$

ν	$\text{NIM}_{P=0.5}$	$\text{NIM}_{p=0.7}$	$\text{NIM}_{P=1.0}$	Exact	$\text{Error}_{p=0.5}$	$\text{Error}_{p=0.7}$	$\text{Error}_{p=1.0}$
0.	−0.146363	−0.154316	−0.161088	−0.161088	0.0147247	0.00677212	3.6923135×10^{-7}
0.1	−0.168856	−0.176569	−0.18312	−0.18312	0.0142638	0.00655108	3.025555×10^{-7}
0.2	−0.190604	−0.19805	−0.20436	−0.20436	0.013756	0.00630954	2.365642×10^{-7}
0.3	−0.21154	−0.218699	−0.22475	−0.22475	0.0132095	0.00605131	1.732927×10^{-7}
0.4	−0.231612	−0.238464	−0.244244	−0.244244	0.0126327	0.00578021	1.143692×10^{-7}
0.5	−0.250776	−0.25731	−0.26281	−0.26281	0.0120338	0.00549997	6.098443×10^{-8}
0.6	−0.269005	−0.275211	−0.280425	−0.280425	0.0114205	0.00521412	1.389851×10^{-8}
0.7	−0.28628	−0.292155	−0.297081	−0.297081	0.0108001	0.00492595	2.652123×10^{-8}
0.8	−0.302596	−0.308137	−0.312776	−0.312776	0.0101794	0.00463842	6.024345×10^{-8}
0.9	−0.317955	−0.323165	−0.327519	−0.327519	0.00956408	0.00435418	8.750504×10^{-8}
1.	−0.332369	−0.337253	−0.341329	−0.341329	0.00895943	0.0040755	1.087412×10^{-7}

By the NIM algorithm, the final solution is under (Figures 5 and 6):

$$\psi(\nu, \sigma) = \psi_0(\nu, \sigma) + \psi_1(\nu, \sigma) + \psi_2(\nu, \sigma) + \cdots, \tag{54}$$

$$\begin{aligned}\psi(\nu, \sigma) = {} & \frac{1}{2e^{\nu} + 1} - \frac{1}{2} + \frac{e^{\nu}\sigma^{p}}{2(2e^{\nu} + 1)^2\Gamma(p + 1)} \\ & + \frac{e^{\nu}\sigma^{2p}}{8(2e^{\nu} + 1)^7}\left(\frac{2e^{2\nu}(2e^{\nu} - 1)\sigma^{2p}\Gamma(3p + 1)}{\Gamma(p + 1)^3\Gamma(4p + 1)}\right. \\ & - \frac{e^{\nu}(2e^{\nu} + 1)(4e^{\nu}(e^{\nu} - 2) + 1)\sigma^{p}\Gamma(2p + 1)}{\Gamma(p + 1)^2\Gamma(3p + 1)} \\ & \left. + \frac{(2e^{\nu} - 1)(2e^{\nu} + 1)^4}{\Gamma(2p + 1)}\right) + \cdots.\end{aligned} \tag{55}$$

Particular attention should be paid to the impacts of 0.5, 0.7, and 1.0 orders when comparing the results obtained with the LRPSM with those obtained with the NIM for Example 2. Importantly, there is a clear pattern: the approximate solution and its reliability both improve as the fractional order p approaches 1. Extensive computational studies are conducted to guarantee the precision of the procedures used in Example 2. The meticulously compiled results of these computations are shown in Tables 5–8. This neatly compiled data set provides substantial evidence for the convergence behavior and overall accuracy of the selected approaches.

4 Conclusion

In conclusion, our study has proven that the LRPSM and the NIM are equally effective and versatile in resolving complex partial differential equations incorporating the Caputo operator. We have successfully developed approximate and effective solutions to the foam drainage equation and the nonlinear time-fractional Fisher's equation, bringing fresh insights into the behavior of these complicated mathematical models. The accuracy of our method is further proved by the use of figures and tables to exemplify it. This work not only enhances the area of mathematical analysis but also emphasizes how vital it is to examine novel approaches to tough difficulties in a range of scientific domains. Our findings illustrate the potential of the NIM and the LRPSM as viable approaches for solving fractional partial differential equations. Combining these methodologies gives a robust strategy for dealing with fractional derivative equations and nonlinear dynamics, boosting our analytical ability to represent real-world events. Our grasp of intricate systems will develop as we use these tactics, and our ability to solve tough mathematical and physical challenges will grow.

In summary, this study underlines the usefulness of unique ways of addressing mathematical problems and encourages greater research into the LRPSM and the NIM for a broader variety of challenges. The foam drainage equation and the nonlinear time-fractional Fisher's equation have been successfully solved, revealing the potential of these methodologies and opening the way for future breakthroughs in mathematical research and its various applications.

Acknowledgments: The authors acknowledge Princess Nourah bint Abdulrahman University Researchers Supporting Project number (PNURSP2023R183), Princess Nourah bint Abdulrahman University, Riyadh, Saudi Arabia. This work was supported by the Deanship of Scientific Research, the Vice Presidency for Graduate Studies and Scientific Research, King Faisal University, Saudi Arabia (Grant No. 4242).

Funding information: Princess Nourah bint Abdulrahman University Researchers Supporting Project number

(PNURSP2023R183), Princess Nourah bint Abdulrahman University, Riyadh, Saudi Arabia. This work was supported by the Deanship of Scientific Research, the Vice Presidency for Graduate Studies and Scientific Research, King Faisal University, Saudi Arabia (Grant No. 4242).

Author contributions: All authors have accepted responsibility for the entire content of this manuscript and approved its submission.

Conflict of interest: The authors state no conflict of interest.

Data availability statement: All data generated or analysed during this study are included in this published article.

References

[1] Alshehry AS, Yasmin H, Ahmad MW, Khan A. Optimal auxiliary function method for analyzing nonlinear system of Belousov-Zhabotinsky equation with Caputo operator. Axioms. 2023;12(9):825.

[2] Hu XB, Wu YT. Application of the Hirota bilinear formalism to a new integrable differential-difference equation. Phys Lett A. 1998;246(6):523–9.

[3] Guo C, Hu J, Wu Y, Čelikovskć S. Non-singular fixed-time tracking control of uncertain nonlinear pure-feedback systems with practical state constraints. IEEE Trans Circuits Syst I Regular Papers. 2023;70(9):3746–58. doi: https://doi.org/10.1109/TCSI.2023.3291700.

[4] Wang M, Zhou Y, Li Z. Application of a homogeneous balance method to exact solutions of nonlinear equations in mathematical physics. Phys Lett A. 1996;216(1–5):67–75.

[5] Yasmin H, Aljahdaly NH, Saeed AM, Shah R. Investigating symmetric soliton solutions for the fractional coupled Konno-Onno system using improved versions of a novel analytical technique. Mathematics. 2023;11(12):2686.

[6] Adomian G. Nonlinear dissipative wave equations. Appl Mathe Lett. 1998;11(3):125–6.

[7] Adomian G, Rach R. Modified decomposition solution of linear and nonlinear boundary-value problems. Nonlinear Anal Theory Meth Appl. 1994;23(5):615–9.

[8] Guo C, Hu J, Hao J, Čelikovskć S, Hu X. Fixed-time safe tracking control of uncertain high-order nonlinear pure-feedback systems via unified transformation functions. Kybernetika. 2023;59(3):342–64. doi: https://doi.org/10.14736/kyb-2023-3-0342.

[9] Yasmin H, Aljahdaly NH, Saeed AM, Shah R. Investigating families of soliton solutions for the complex structured coupled fractional Biswas-Arshed model in birefringent fibers using a novel analytical technique. Fractal Fractional. 2023;7(7):491.

[10] Karmishin AV, Zhukov AI, Kolosov VG. Methods of dynamics calculation and testing for thin-walled structures. Mashinostroyenie, Moscow, Russia; 1990.

[11] Liao SJ. On the proposed homotopy analysis technique for nonlinear problems and its applications. Shanghai Jiao Tong University; 1992.

[12] Liao SJ. An explicit, totally analytic approximate solution for Blasius' viscous flow problems. Int J Non-Linear Mech. 1999;34(4):759–78.

[13] Yasmin H, Aljahdaly NH, Saeed AM, Shah R. Probing families of optical soliton solutions in fractional perturbed Radhakrishnan-Kundu-Lakshmanan model with improved versions of extended direct algebraic method. Fract Fract. 2023;7(7):512.

[14] Liao SJ. A general approach to get series solution of non-similarity boundary-layer flows. Commun Nonlinear Sci Numer Simulat. 2009;14(5):2144–59.

[15] Liao S. On the homotopy analysis method for nonlinear problems. Appl Math Comput. 2004;147(2):499–513.

[16] Liao S. A new branch of solutions of boundary-layer flows over an impermeable stretched plate. Int J Heat Mass Transfer. 2005;48(12):2529–39.

[17] Li Q, Lin H, Tan X, Du SH. infty consensus for multiagent-based supply chain systems under switching topology and uncertain demands. IEEE Trans Syst Man Cybernetic Syst. 2020;50(12):4905–18. doi: https://doi.org/10.1109/TSMC.2018.2884510.

[18] Molabahrami A, Khani F. The homotopy analysis method to solve the Burgers-Huxley equation. Nonlinear Anal Real World Appl. 2009;10(2):589–600.

[19] Jin H, Wang Z. Boundedness, blowup and critical mass phenomenon in competing chemotaxis. J. Differ. Equ. 2016;260(1):162–96. doi: https://doi.org/https://doi.org/10.1016/j.jde.2015.08.040.

[20] Khani F, Raji MA, Hamedi-Nezhad S. A series solution of the fin problem with a temperature-dependent thermal conductivity. Commun Nonlinear Sci Numer Simulat. 2009;14(7):3007–17.

[21] Khani F, Farmany A, Raji MA, Aziz A, Samadi F. Analytic solution for heat transfer of a third grade viscoelastic fluid in non-Darcy porous media with thermophysical effects. Commun Nonlinear Sci Numer Simulat. 2009;14(11):3867–78.

[22] Liu P, Shi J, Wang ZA. Pattern formation of the attraction-repulsion Keller-Segel system. Discrete Contin Dyn Syst B. 2013;18(10):2597–625. doi: https://doi.org/10.3934/dcdsb.2013.18.2597.

[23] Jin H, Wang Z, Wu L. Global dynamics of a three-species spatial food chain model. J Differ Equ. 2022;333:144–83. doi: https://doi.org/10.1016/j.jde.2022.06.007.

[24] Li D, Ge SS, Lee TH. Fixed-time-synchronized consensus control of multiagent systems. IEEE Trans Control Netw Syst. 2021;8(1):89–98. doi: https://doi.org/10.1109/TCNS.2020.3034523.

[25] Ma Q, Meng Q, Xu S. Distributed optimization for uncertain high-order nonlinear multiagent systems via dynamic gain approach. IEEE Trans Syst Man Cybernetics Syst. 2023;53(7):4351–7. doi: https://doi.org/10.1109/TSMC.2023.3247456.

[26] Stone HA, Koehler SA, Hilgenfeldt S, Durand M. Perspectives on foam drainage and the influence of interfacial rheology. J Phys Condensed Matter. 2002;15(1):S283.

[27] Hilgenfeldt S, Koehler SA, Stone HA. Dynamics of coarsening foams: accelerated and self-limiting drainage. Phys Rev Lett 20018;6(20):4704.

[28] Fisher RA. The wave of advance of advantageous genes. Ann Eugenics. 1937;7(4):355–69.

[29] Frank-Kamenetskii DA. Diffusion and heat exchange in chemical kinetics. Vol. 2171. New Jersey: Princeton University Press; 2015.

[30] Ammerman AJ, Cavalli-Sforza LL. Measuring the rate of spread of early farming in Europe. Man. 1971;6:674–88.

[31] Bramson MD. Maximal displacement of branching Brownian motion. Commun Pure Appl Math. 1978;31(5):531–81.
[32] Canosa J. Diffusion in nonlinear multiplicative media. J Math Phys. 1969;10(10):1862–8.
[33] Wang XY. Exact and explicit solitary wave solutions for the generalised Fisher equation. Phys Lett A. 1988;131(4–5):277–9.
[34] Branco JR, Ferreira JA, De Oliveira P. Numerical methods for the generalized Fisher-Kolmogorov-Petrovskii-Piskunov equation. Appl Numer Math. 2007;57(1):89–102.
[35] Macias-Diaz JE, Medina-Ramirez IE, Puri A. Numerical treatment of the spherically symmetric solutions of a generalized Fisher-Kolmogorov-Petrovsky-Piscounov equation. J Comput Appl Math. 2009;231(2):851–68.
[36] Wazwaz AM, Gorguis A. An analytic study of Fisher's equation by using Adomian decomposition method. Appl Math Comput. 2004;154(3):609–20.
[37] Polyanin AD, Zaitsev VF. Handbook of Nonlinear Partial Differential Equations. Boca Raton: CRC Press; 2004.
[38] Gu H, Lou B, Zhou M. Long time behavior of solutions of Fisher-KPP equation with advection and free boundaries. J Funct Anal. 2015;269(6):1714–68.
[39] El-Ajou A. Adapting the Laplace transform to create solitary solutions for the nonlinear time-fractional dispersive PDEs via a new approach. Europ Phys J Plus. 2021;136(2):1–22.
[40] El-Tantawy SA, Shah R, Alrowaily AW, Shah NA, Chung JD, Ismaeel SM. A comparative study of the fractional-order Belousov–Zhabotinsky system. Mathematics. 2023;11(7):1751.
[41] Alquran M, Ali M, Alsukhour M, Jaradat I. Promoted residual power series technique with Laplace transform to solve some time-fractional problems arising in physics. Results Phys. 2020;19:103667.
[42] Naeem M, Yasmin H, Shah R, Shah NA, Nonlaopon K. Investigation of fractional nonlinear regularized long-wave models via Novel techniques. Symmetry. 2023;15(1):220.
[43] Jawarneh Y, Yasmin H, Al-Sawalha MM, Khan A. Fractional comparative analysis of Camassa-Holm and Degasperis-Procesi equations. AIMS Math. 2023;8(11):25845–62.
[44] Kbiri Alaoui M, Nonlaopon K, Zidan AM, Khan A, Shah R. Analytical investigation of fractional-order Cahn-Hilliard and Gardner equations using two novel techniques. Mathematics 2022;10(10):1643.
[45] Zidan AM, Khan A, Shah R, Alaoui MK, Weera W. Evaluation of time-fractional Fisher's equations with the help of analytical methods. Aims Math. 2022;7(10):18746–66.
[46] Shafee A, Alkhezi Y, Shah R. Efficient solution of fractional system partial differential equations using Laplace residual power series method. Fract Fract. 2023;7(6):429.
[47] Alkhezi Y, Shafee A, Shah R. Fractional view analysis of partial differential equation via residual power series transform method. Appl Math Sci. 2022;16(12):585–99.
[48] Alaroud M. Application of Laplace residual power series method for approximate solutions of fractional IVPas. Alexandr Eng J. 2022;61(2):1585–95.
[49] Bhalekar S, Daftardar-Gejji V. New iterative method: application to partial differential equations. Appl Math Comput. 2008;203(2):778–83.
[50] Jafari H, Nazari M, Baleanu D, Khalique CM. A new approach for solving a system of fractional partial differential equations. Comput Math Appl. 2013;66(5):838–43.
[51] Falade KI, Tiamiyu AT. Numerical solution of partial differential equations with fractional variable coefficients using new iterative method (NIM). IJ Math Sci Comput. 2020;3:12–21.